Angewandte Chemie
GDCh
Eine Zeitschrift der Gesellschaft Deutscher Chemiker
www.angewandte.de

Akzeptierter Artikel

Titel: Robust DNA-bridged memristor for textile chip

Autoren: Xiaojie Xu, Xufeng Zhou, Tianyu Wang, Xiang Shi, Ya Liu, Yong Zuo, Limin Xu, Mengying Wang, Xiaofeng Hu, Xinju Yang, Jiaxin Chen, Xiubo Yang, Lin Chen, Peining Chen, and Huisheng Peng

Zitierweise: *Angew. Chem. Int. Ed.* 10.1002/anie.202004333

Link zur VoR: https://doi.org/10.1002/anie.202004333

WILEY-VCH

10.1002/ange.202004333

Robust DNA-bridged memristor for textile chip

Xiaojie Xu[+], Xufeng Zhou[+], Tianyu Wang[+], Xiang Shi, Ya Liu, Yong Zuo, Limin Xu, Mengying Wang, Xiaofeng Hu, Xinju Yang, Jiaxin Chen, Xiubo Yang, Lin Chen, Peining Chen, Huisheng Peng**

Dr. X. Xu,[+] X. Zhou,[+] X. Shi, Y. Zuo, L, Xu, M. Wang, Prof. P. Chen, Prof. H. Peng
State Key Laboratory of Molecular Engineering of Polymers, Department of Macromolecular Science, and Laboratory of Advanced Materials, Fudan University, Shanghai 200438, China; E-mail: penghs@fudan.edu.cn.

T. Wang,[+] Prof. L. Chen
State Key Laboratory of ASIC and System, School of Microelectronics, Fudan University, Shanghai 200433, China; E-mail: linchen@fudan.edu.cn.

Y. Liu
International Research Center for Renewable Energy, State Key Laboratory of Multiphase Flow in Power Engineering, Xi'an Jiao Tong University, Shannxi 710049, China.

X. Hu, X. Yang
State Key Laboratory of Surface Physics, Fudan University, Shanghai 200438, China.

J. Chen
Department of Materials Science, Fudan University, Shanghai 200438, China.

X. Yang
Analytical & Testing Center, Northwestern Polytechnical University, Shaanxi 710072, China.

[+]*These three authors contributed equally to this work.*

***Abstract*:** *Electronic textiles that are thin, lightweight, flexible and breathable have been widely explored with a variety of functionalities including power supplying, displaying and sensing, which may revolutionize many fields such as communication, health care and artificial intelligence. To date, unfortunately, computing is the missing puzzle to close their functional loop. Memristor is compatible with the interwoven structure and fabricating process in textile due to its two-terminal crossbar configuration. However, it remains challenging to realize textile memristors due to the*

10.1002/ange.202004333

difficulties in designing advanced memristive materials and achieving high-quality active layers on fiber electrodes. Here we report a robust textile memristor based on an electrophoretic-deposited active layer of deoxyribonucleic acid (DNA) on fiber electrodes. The unique architecture and orientation of DNA molecules with the incorporation of Ag nanoparticles offer the best-in-class performances, e.g., both ultra-low operation voltage of ~0.3 V and power consumption of ~100 pW and high switching speed of 20 ns. Fundamental logic calculations such as implication and NAND are demonstrated as functions of textile chips, and it has been thus integrated with power-supplying and light emitting modules to demonstrate an all-fabric information processing system. This work provides a promising route towards wearable information processing and artificial neural networks for effective brain-machine interfaces.

Electronic textiles have embraced a great boost in the past decade, from power sources to sensors and to displays, which may produce the long-cherished soft electronics to revolutionize a variety of application fields such as information technology, internet of things, artificial intelligence and personal healthcare. [1-4] The core of electronic textiles is to replace the building block of traditional polymer fibers with electronic fibers and then integrate the electronic fibers into textiles by the scalable weaving process.[5] However, one key component, i.e., the data-processing system, remains far less developed to close the functional loop of electronic textiles. In other words, computing is the missing puzzle from the full picture of electronic textiles.

Memristor, a promising candidate for next-generation computing,[6-10] is compatible with the interwoven architecture of textile owing to its two-terminal and cross-bar configuration. The rigid silicon substrate and lithography patterned electrode can thus be replaced with flexible fiber electrodes.[11] A variety of memristive materials, such as metal oxides,[6,7] chalcogenides[12-14] and organic materials,[15-17] have been explored as active layers for memristors. Among them, organic materials have attracted growing interests due to their chemically tunable functionality, solution processability and intrinsic flexibility, which can serve as promising candidates for large-scale fabrications of textile memristors.[18] However, they suffer from severe limitations in memristive performances such as low switching speed, high operation voltage and insufficient stability.[15,18] To the best of our knowledge, there are not robust textile memristors due to the bottlenecks of materials design and active layer fabrication, e.g., it is critical while difficult to make a rational organization of building molecules to guide the effective formation of conductive filaments for efficient ion transport; it is of course more difficult to achieve uniform active layers with nanometer thicknesses at curved surfaces of fiber electrodes that range from several to hundreds of micrometers.

In this report, we discover deoxyribonucleic acid (DNA),[19,20] a bio-compatible material and good ionic conductor with a double helix chain, could serve as an active material for robust memristors. The DNA molecules are assembled into a continuous and uniform film at nanometer scale on flexible metal fibers *via* electrophoretic deposition, which is demonstrated as a promising method for effective deposition on conductive substrates.[21,22] They thus can be interlaced with another kind of fiber electrodes to produce textile chips (Figure 1a). The contact point between the DNA-deposited electrode and another flexible metal fiber functions as a memristor unit, which demonstrates superior memristive performances – ultra-low operation voltage (~0.3 V), high switching speed (20 ns) and low power consumption (~100 pW) – to previously reported organic memristors (Supplementary Information, Table S1). It is found that the orientation of DNA molecules plays a vital role in robust performance by providing an efficient highway for filament growth.

In a typical preparation, two parallel electrodes were immersed in a solution containing DNA molecules and surfactants (Supplementary Information, Figure S1). Upon applying an external electric field of 1.8 V for 3 min, the negatively charged DNA molecules would move towards the positive electrode due to electrostatic attraction and assemble into a conformal thin film.[23] As shown in Figure 1b, a thin and uniform DNA film was continuously deposited onto the Ag fiber anode. Energy-dispersive X-ray spectroscopy showed that C, N and P are homogeneously and densely distributed (Figure 1d-f), indicating that DNA molecules were successfully assembled on the Ag fiber. The thicknesses of DNA films could be readily tuned in a range of tens to hundreds of nanometers by changing applied voltage and deposition time. The DNA film with an optimized thickness of ~50 nm is shown in Figure. 1g and 1h. Raman spectra further verified the effective deposition since the characteristic peaks of DNA were clearly detected[23] (Supplementary Information, Figure S2). As shown in Figure 1c, we found that Ag nanoparticles (AgNPs) as a form of tiny bulges were uniformly distributed in the DNA film. In other words, AgNPs were simultaneously deposited with DNA molecules into the film. Transmission electron microscopy indicated that the AgNPs showed an average diameter of ~3 nm (Figure 1h). The small size of AgNPs was attributed to the use of surfactants that could prevent AgNPs from aggregation during the assembling process[21]. High-resolution transmission electron microscopy images in Figure 1i and Supplementary Information, Figure S3 also demonstrated the effective incorporation of AgNPs. It is further verified by X-ray photoelectron spectroscopy as almost no oxidation peaks of Ag were observed (Supplementary Information, Figure S4). Capacitance–voltage measurements were also carried out to investigate the incorporation of DNA and AgNPs. An obvious oxidation and reduction process of Ag was observed during the assembling process (Supplementary Information, Figure S5), indicating the formation of Ag^+ due to the oxidation at the surface of Ag electrode under electrical field. The Ag^+ would subsequently bind to the DNA molecules due to

10.1002/ange.202004333

their high electron affinity to the base pairs (e.g., G-guanine and C-cytosine),[24,25] and the Ag^+ were then readily reduced by the guanine free radicals to AgNPs.[24] The DNA molecules decorated with the AgNPs thus form a thin and continuous film on the electrode under electrical field. Fourier transform infrared spectroscopy showed characteristic peaks at 1088 cm^{-1} for phosphate symmetric stretching and 1222 cm^{-1} for PO_2 asymmetric stretching in the DNA backbones[26,27] (Supplementary Information, Figure S6), which is consistent with the results from Raman spectra[28]. The variations of the relative peak intensities of base pairs at 1663 cm^{-1} (Thymine: C_2=O stretching) and 1717 cm^{-1} (Guanine: C=O stretching) suggested a chemical interaction occurs between AgNPs and DNA molecules.[23,26]

A flexible memristor can be fabricated by interlacing the modified Ag fiber with a Pt fiber. Upon applying a direct current sweep, the resulting textile memristor demonstrated a typical bipolar memristive switching behavior (Figure 2a). It exhibited a high stability since no obvious variations were observed after 50 cycles of direct current sweeps. The voltage of the first set cycle was the same as that of the normal operation setting, indicating that no pre-electroforming process was required for device operation. As shown in Figure 2b, a very low operating voltage (~0.3 V) with narrow distribution was needed to program and erase, indicating an operation uniformity of the DNA memristor. The memristor could be switched within 20 ns *via* a low voltage (Figure 2c), which is comparable to those of the state-of-art planar memristors.[14,15,29-31] The conductance state could be well maintained under a broad reading pulse. Besides, the memristor exhibited a long retention time of more than 10^5 s both under high and low resistance states (Figure 2d). Upon applying a constant voltage on the device, the ratio between high and low resistance states exceeded 10^6 (Figure 2e) and was then well maintained after thousands of switching cycles. The ultra-low operation voltage (0.3 V) and ultra-high switching speed (20 ns) are comparable to the state-of-art metal oxide memristors,[30] and the ultra-low power consumption and high on-off ratio have been rarely reported for organic memristors[16,17,32-35] (Figure 2f and Supplementary Information Table S1).

Based on the experimental results, a working mechanism is proposed in Figure 3a. The grazing-incidence small-angle scattering patterns verify that the DNA/AgNP film prepared by electrophoretic deposition showed an oriented structure (Figure 3b).[22,36] That is, an oriented arrangement of DNA chains is formed in the active layer during the electrophoretic deposition, which is crucial for the low operation voltage and high switching speed, because the orientation of DNA molecules could provide effective ionic pathways for Ag^+ transport when set voltage is applied.[36,37]

10.1002/ange.202004333

We carefully investigated the assembly structure of the DNA/AgNP film to verify the above mechanism. At the virgin state, the AgNPs were evenly distributed in the DNA film (Figure 3c). Once set, the Ag filament bridged over the two electrodes and showed a preferential orientation to the substrate (Figure 3d**)**, indicating the orientated DNA chains were capable of incorporating with AgNPs to guide the growth of filaments. The current mapping through *in-situ* conductive atomic force microscopy also suggested that multiple conductive filaments were formed and annihilated upon set and reset switching, respectively (Supplementary Information, Figure S7). In comparison, the DNA film prepared *via* dip-coating demonstrated a homogeneous structure (Figure 3e). The resulting memristor exhibited a much higher operation voltage than that with an oriented arrangement of DNA chains (Figure 3f). Besides, the set speed of the former was approximately two orders of magnitude slower than the latter (Figure 3g and Supplementary Information, Figure S8).

The small-area Fourier transform infrared spectroscopy was further employed to study the chemical bonding information of the active switching area (Supplementary Information, Figure S9). The increased intensity at 1715 cm^{-1} when the device was set suggested a strong vibration of C=O bonds from the nucleic base pairs, indicating a strong interaction between Ag^+ and base pairs of DNA. The oriented DNA molecules could induce filament growth along the DNA chains through the pre-anchored AgNPs. As expected, the counterpart device with the architecture of Pt/DNA/Ag, lacking pre-anchored AgNPs, showed a higher operation voltage of 0.6 V (Supplementary Information, Figure S10 and S11). In other words, the oriented arrangement of DNA chains enabled effective ionic pathways for Ag^+ migration between the two electrodes. [38,39] The pre-anchored AgNPs can lower the nucleation barrier and concentrate the local electrical field to further reduce the switching voltages.[14] This strategy may be extended to the other organic materials with high ionic conductivities such as silk polymers.

Due to the high performance and simple fabrication of DNA-bridged memristors, the textile chip could be easily produced by weaving DNA-deposited Ag fibers with Pt fibers, and it could thus be integrated with power-supplying and light-emitting modules to realize proof-of-concept fabric data-processing system (Figure 4a). As shown in Figure 4b, basic logic gates including implication (IMP) and NAND were demonstrated through the as-fabricated textile chip. For IMP operation, two memristors were connected in parallel, followed by one fixed load resistor in series. By integrating logic and memory function, the nonvolatile logic-in-memory circuit was realized *via* IMP logic architecture, which is important as it can complete computing logic basis together with FALSE operation. The logic computation from a combination of a set of logic operations relies on the number of devices and the sequence of variables in IMP. In this design, a low resistance state of the device was used to stand for a logic 1, and a high resistance state stood for a logic 0. Upon

applying set pulse of 0.4 V and reference pulse of 0.2 V to Devices A and B, respectively, they were switched to A' and B' based on their previous resistances to realize IMP functions. The logic value of B depended on that of A. If A=logic 0, then this logic operation always generated output B'=logic 1; if A=logic 1, then B' is left unchanged. The implementation of IMP operation is shown in Figure 4c. As a universal logic operation, NAND was performed with three memristors and one fixed load resistor with two steps (Figure 4d). Firstly, pulses of 0.4 and 0.2 V were applied to Devices A and C, respectively. Then, pulses of 0.4 and 0.2 V were used for Devices B and C, respectively. With modulation of initial resistance states of Devices A, B and C, the four kinds of logic operations of NAND were verified. To ensure C=0, "FALSE C" was operated *via* applied reset voltage to device C. Then, "NOT A" logic operation was realized through "A IMP C" with the output of C'. Next, "B IMP C'" was implemented to generate the final state of C''. The output C'' was logic 0 only when AB = 11, which represented the logic operation of C'' = A NAND B.

The woven textile chip could be further integrated with the textile power source and light-emitting modules to realize a wearable information processing system (Figure 4e). Photovoltaic fibers for electricity generation (Supplementary Information, Figure S12 and S13) and fiber-shaped batteries for electricity storage (Supplementary Information, Figure S14 and S15) were woven and connected in series with the memristors. A voltage transformer was used to supply a pulsed bias, so the conductance state of the memristor can be switched and memorized. Multiple Ag metal wires coated with DNA films were woven with Pt metal wires into a fabric module for the "logic-in-memory-computing". Electroluminescent fibers were also woven into the textile to work as a basic component to display the processed information (Supplementary Information, Figure S16 and S17). By applying different pulses and combinations, "information" was input to the system. The pulses were transmitted to each memristor unit (contact point) through parallel controllers. Each memristor would respond to the pulse intensity and be summed, which was considered as "information processing". Besides, the output current was then transmitted to the controller to initiate the light-emitting fibers to turn on or off. The all-fabric information processing system was lightweight, soft and breathable like normal fabrics.

In summary, we discover that DNA can serve as a new and promising material to produce novel textile memristors for logic circuits at a large scale. The oriented DNA molecules incorporated with Ag nanoparticles were found to guide the filament growth for a low operation voltage, low operation power and high switching speed. The design of DNA molecules for the active layer and realization of textile memristors with high performances provide new directions in the development of the next-generation memristors and textile electronics.

Supplementary Information

Supporting Information is available from the Wiley Online Library or from the author.

Acknowledgements

The authors appreciated the helpful discussions and intellectual contributions from Dr. Christine Orme. This work was supported by MOST (2016YFA0203302), NSFC (21634003, 51573027, 21805044), STCSM (16JC1400702, 19QA1400800) and SHMEC (2017-01-07-00-07-E00062).

Author Contributions

H. P. and X. X. conceived the idea and designed the experiment. X. X., X. Z. and T. W. performed the experiments and contributed equally to this work. X. X. and X. Z. fabricated the DNA memristors and cross-bar arrays, characterized the morphology, assembly structure, and electrical properties and switching mechanism. T. W. and L. C. tested the memristive switching behaviors and realized the basic logic calculations including IMP and NAND. X. Z., X.X., X. S., Y. Z., L. X., and M. W. realized the proof-of-concept textile fabric information processing system. Y. L and X. Y. performed the TEM measurement. X. H. and Q. Y. performed the conductive atomic force microscopy. All the authors participated in analyzing the data and preparing the manuscript.

Conflict of interest

The authors declare no conflict of interest.

References

[1] H. Sun, Y. Zhang, J. Zhang, X. Sun, H. Peng, *Nat. Rev. Mater.* **2017**, *2*, 17023.
[2] M. Rein, V. D. Favrod, C. Hou, T. Khudiyev, A. Stolyarov, J. Cox, C.-C. Chung, C. Chhav, M. Ellis, J. Joannopoulos, Y. Fink, *Nature* **2018**, *560*, 214–218.
[3] S. Shabahang, G. Tao, J. J. Kaufman, Y. Qiao, L. Wei, T. Bouchenot, A. P. Gordon, Y. Fink, Y. Bai, R. S. Hoy, A. F. Abouraddy, *Nature* **2016**, *534*, 529–533.
[4] X. Wu, H. Peng, *Science Bulletin* **2019**, *64*, 634-640.
[5] X. Xu, S. Xie, Y. Zhang, H. Peng, *Angew. Chem. Int. Ed.* **2019**, *58*, 13643–13653.
[6] D. B. Strukov, G. S. Snider, D. R. Stewart, R. S. Williams, *Nature* **2008**, *453*, 80–83.
[7] Z. Wang, S. Joshi, S. E. Savel'ev, H. Jiang, R. Midya, P. Lin, M. Hu, N. Ge, J. P. Strachan, Z. Li, Z. Li, Q. Wu, M. Barnell, G-L. Li, H. L. Xin, R. S. Williams, Q. Xia; J. J. Yang, *Nat. Mater.* **2017**, *16*, 101–108.

[8] M. A. Zidan, J. P. Strachan, W. D. Lu, *Nat. Electron.* **2018**, *1*, 22–29.
[9] C. Li, M. Hu, Y. Li, H. Jiang, N. Ge, E. Montgomery, J. Zhang, W. Song, N. Dávila, C. E. Graves, Z. Li, J. P. Strachan, P. Lin, Z. Wang, M. Barnell, Q. Wu, R. S. Williams, J. J. Yang, Q. Xia, *Nat. Electron.* **2018**, *1*, 52–59.
[10] P. M. Sheridan, F. Cai, C. Du, W. Ma, Z. Zhang, W. D. Lu, *Nat. Nanotechnol.* **2017**, *12*, 784–789.
[11] M. Hamedi, R. Forchheimer, O. Inganäs, *Nat. Mater.* **2007**, *6*, 357–362.
[12] Y. Zhai, X. Yang, F. Wang, Z. Li, G. Ding, Z. Qiu, Y. Wang, Y. Zhou, S. T. Han, *Adv. Mater.* **2018**, *30*, 1803563.
[13] V. K. Sangwan, D. Jariwala, I. S. Kim, K. S. Chen, T. J. Marks, L. J. Lauhon, M. C. Hersam, *Nat. Nanotechnol.* **2015**, *10*, 403–406.
[14] X. Yan, Y. Pei, H. Chen, J. Zhao, Z. Zhou, H. Wang, L. Zhang, J. Wang, X. Li, C. Qin, G. Wang, Z. Xiao, Q. Zhao, K. Wang, H. Li, D. Ren, Q. Liu, H. Zhou, J. Chen, P. Zhou, *Adv. Mater.* **2019**, *31*, 1805284.
[15] S. Goswami, A. J. Matula, S. P. Rath, S. Hedström, S. Saha, M. Annamalai, D. Sengupta, A. Patra, S. Ghosh, H. Jani, S. Sarkar, M. R. Motapothula, C. A. Nijhuis, J. Martin, S. Goswami, V. S. Batista, T. Venkatesan, *Nat. Mater.* **2017**, *16*, 1216–1224.
[16] C. Wu, F. Li, Y. Zhang, T. Guo, T. Chen, *Appl. Phys. Lett.* **2011**, *99*, 042108.
[17] H. Wang, F. Meng, Y. Cai, L. Zheng, Y. Li, Y. Liu, Y. Jiang, X. Wang, X. Chen, *Adv. Mater.* **2013**, *25*, 5498–5503.
[18] Y. Van De Burgt, A. Melianas, S. T. Keene, G. Malliaras, A. Salleo, *Nat. Electron.* **2018**, *1*, 386–397.
[19] M. R. Jones, N. C. Seeman, C. A. Mirkin, *Science.* **2015**, *347*, 1260901.
[20] Z. Chen, C. Liu, F. Cao, J. Ren, X. Qu, *Chem. Soc. Rev.* **2018**, *47*, 4017–4072.
[21] Y. Yu, D. Yu, C. A. Orme, *Nano Lett.* **2017**, *17*, 3862–3869.
[22] Y. Yu, D. Yu, B. Sadigh, C. A. Orme, *Nat. Commun.* **2018**, *9*, 4211.
[23] Wood, B. R. The importance of hydration and DNA conformation in interpreting infrared spectra of cells and tissues. *Chem. Soc. Rev.* **2016**, *45*, 1980–1998.
[24] G. Eidelshtein, N. Fardian-Melamed, V. Gutkin, D. Basmanov, D. Klinov, D. Rotem, Y. Levi-Kalisman, D. Porath, A. Kotlyar, *Adv. Mater.* **2016**, *28*, 4839–4844.
[25] N. Fardian-Melamed, G. Eidelshtein, D. Rotem, A. Kotlyar, D. Porath, *Adv. Mater.* **2019**, *31*, 1902816.
[26] H. Arakawa, J. F. Neault, H. A. Tajmir-Riahi, *Biophys. J.* **2001**, *81*, 1580–1587.
[27] M. L. S. Mello, B. C. Vidal, *PLoS One* **2012**, *7*, e43169.
[28] J. De Gelder, K. De Gussem, P. Vandenabeele, L. Moens, *J. Raman Spectrosc.* **2007**, *38*, 1133–1147.

[29] M. Wang, S. Cai, C. Pan, C. Wang, X. Lian, Y. Zhuo, K. Xu, T. Cao, X. Pan, B. Wang, S-J. Liang, J. J. Yang, P. Wang, F. Miao, *Nat. Electron.* **2018**, *1*, 130–136.
[30] Q. Xia, J. J. Yang, *Nat. Mater.* **2019**, *18*, 309–323.
[31] X. Wu, R. Ge, P. A. Chen, H. Chou, Z. Zhang, Y. Zhang, S. Banerjee, M. H. Chiang, J. C. Lee, D. Akinwande, *Adv. Mater.* **2019**, *31*, 1806790.
[32] Y. C. Chang, Y. H. Wang, *Appl. Phys. Lett.* **2015**, *106*, 123302.
[33] H. F. Ling, M. D. Yi, M. Nagai, L. H. Xie, L. Y. Wang, B. Hu, W. Huang, *Adv. Mater.* **2017**, *29*, 1701333.
[34] Y. Xing, C. Shi, J. Zhao, W. Qiu, N. Lin, J. Wang, X. B. Yan, W. D. Yu, X. Y. Liu, *Small* **2017**, *13*, 1702390.
[35] J. Liu, F. Yang, L. Cao, B. Li, K. Yuan, S. Lei, W. Hu, *Adv. Mater.* **2019**, *31*, 1902264.
[36] J. Wan, J. Xie, X. Kong, Z. Liu, K. Liu, F. Shi, A. Pei, H. Chen, W. Chen, J. Chen, X. Zhang, L. Zong, J. Wang, L-Q. Chen, J. Qin, Y. Cui, *Nat. Nanotechnol.* **2019**, *14*, 705–711.
[37] J. Kondo, Y. Tada, T. Dairaku, Y. Hattori, H. Saneyoshi, A. Ono, Y. Tanaka, *Nat. Chem.* **2017**, *9*, 956–960.
[38] F. Alibart, S. Pleutin, O. Bichler, C. Gamrat, T. Serrano-Gotarredona, B. Linares-Barranco, D. Vuillaume, *Adv. Funct. Mater.* **2012**, *22*, 609–616.
[39] Y. Yang, P. Gao, S. Gaba, T. Chang, X. Pan, W. Lu, *Nat. Commun.* **2012**, *3*, 732–738.

10.1002/ange.202004333

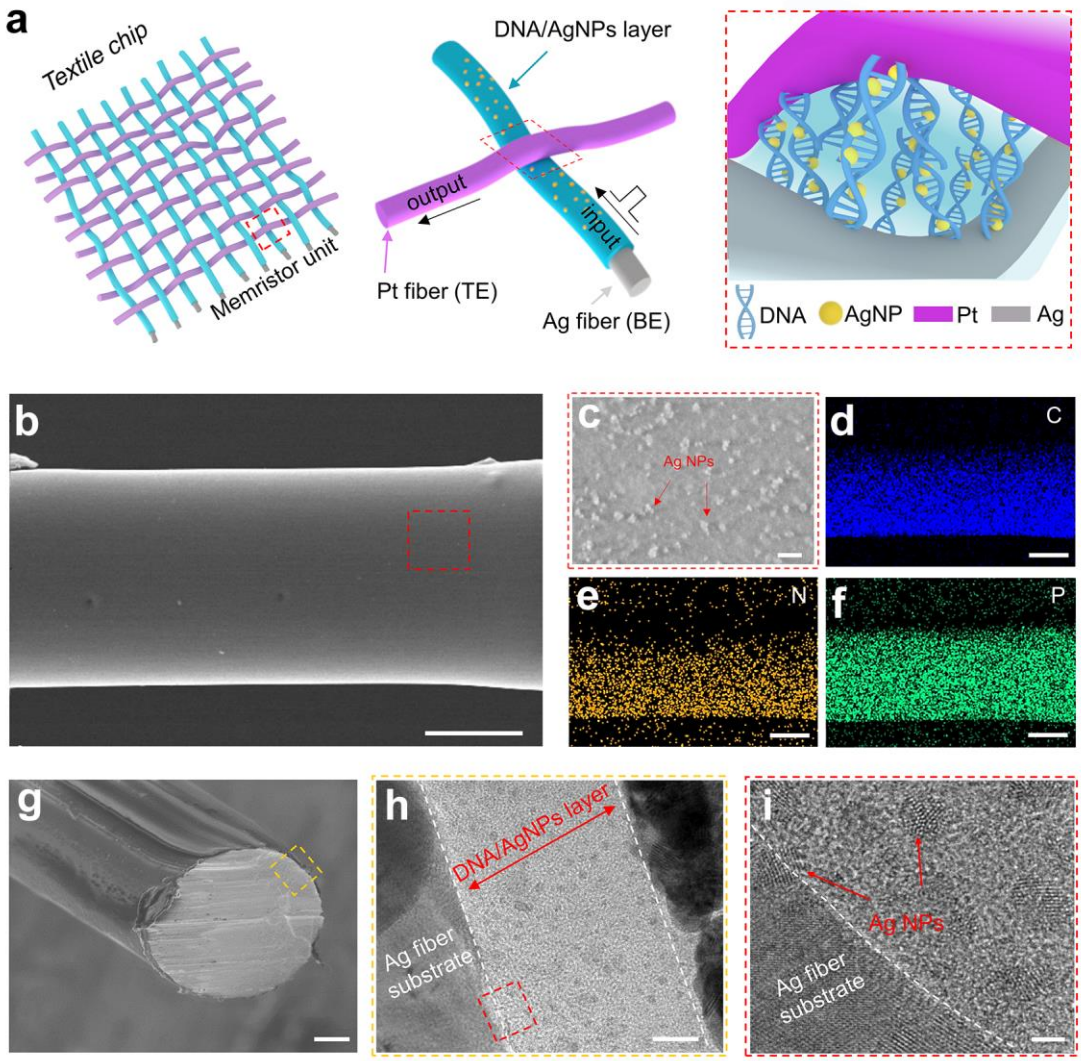

Figure 1. Schematic illustration of robust DNA-bridged memristor for the textile chip. a) Textile chip made from DNA-bridged memristor cross-bar arrays. Each contact point represents a memristor. **b)** SEM image of conformal coating of DNA layer onto Ag fiber *via* electrophoretic deposition with simultaneous modification of AgNPs. **c)** High-resolution scanning electron microscopy image of the surface morphology of the assembled DNA/AgNP layer. **d-f)** Energy-dispersive X-ray spectroscopy mapping of the assembled DNA/AgNPs onto Ag fibre. **g)** Cross-sectional scanning electron microscopy image of a thin and continuous DNA/AgNP layer on the Ag fiber. **h-i)** High-resolution transmission electron microscopy image of DNA layer doped with AgNPs. Scale bars in **b, d, e** and **f is** 20 μm, **c** is 100 nm, **g** is 10 μm, **h** is 10 nm and **i** is 2 nm, respectively.

10.1002/ange.202004333

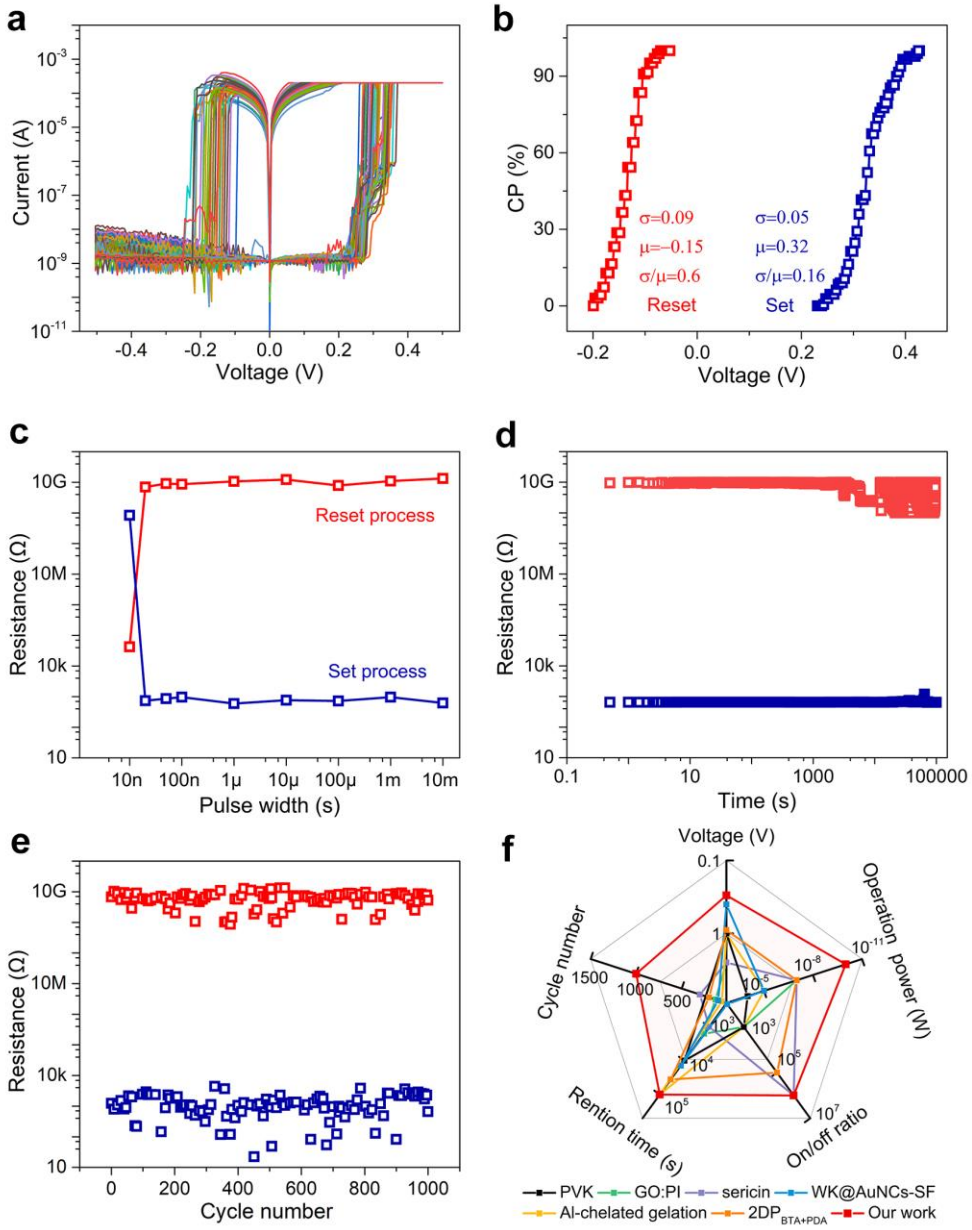

Figure 2. Memristive characteristics of robust DNA-bridged memristor with the interlaced structure. a) Repeatable highly uniform switching *I-V* loops for the DNA-bridged memristor. **b)** Distribution of the set and reset voltages of the DNA-bridged memristor. **c)** High-speed switching characteristics of the DNA-bridged memristor. **d)** Retention time of set and reset states. **e)** Cycling property of the DNA memristor. **f)** Comparison of the memristor performances between DNA-bridged memristor and the state-of-art organic memristors, including PVK (poly(9-vinylcarbazole)[33], GO:PI (graphene oxide sheets/polyimide)[16], Sericin [17] ,WK@AuNCs-SF (wool keratin@ gold nanoclusters - silk fibroin)[34], Al-chelated gelation[32], $2DP_{BTA+PDA}$ (2D imine polymer constructed by benzene-1,3,5-tricarbaldehyde (BTA) and p-phenylenediamine (PDA) precursors)[35].

10.1002/ange.202004333

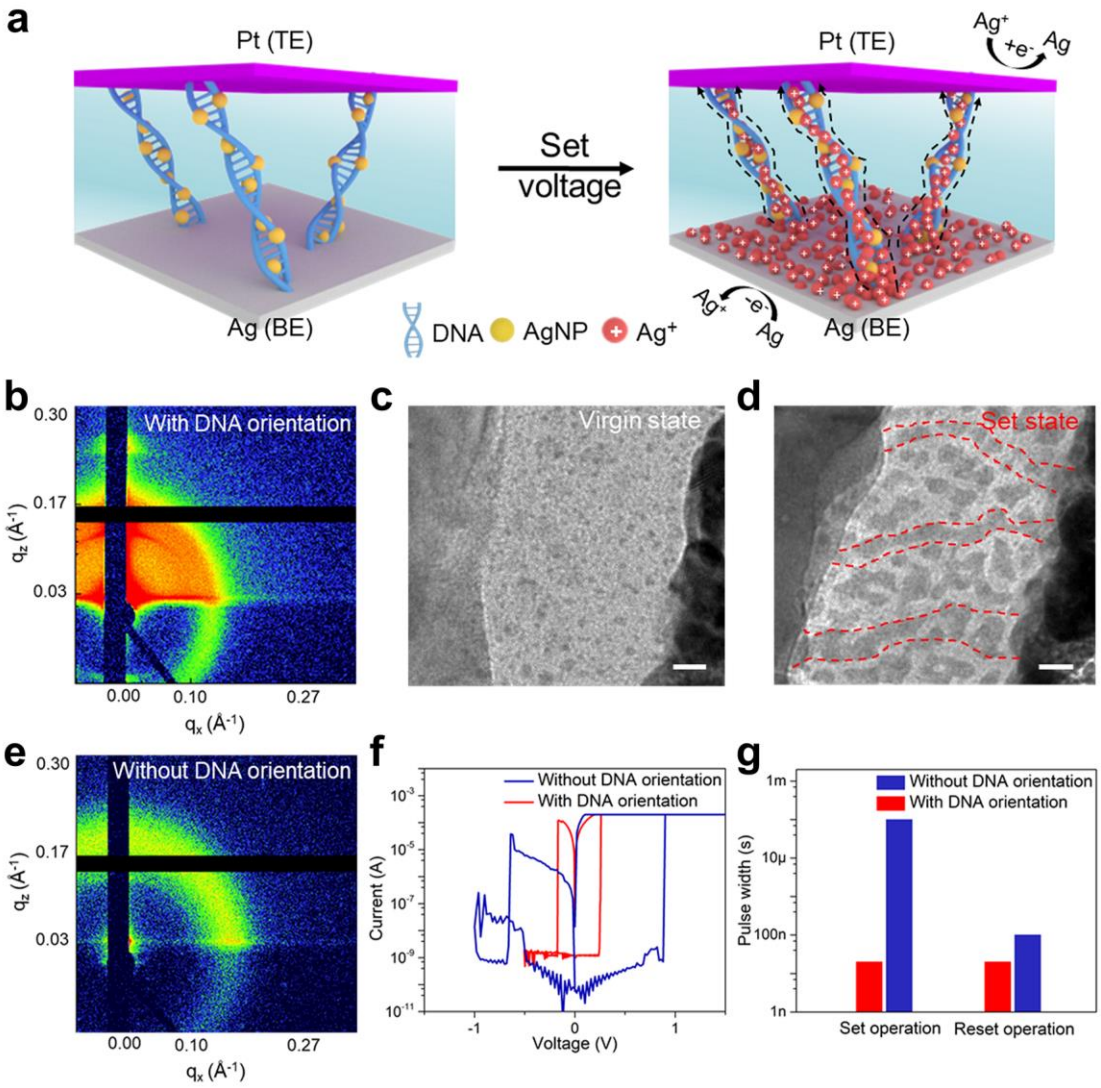

Figure 3. Switching mechanism of robust DNA-bridged memristors. a) Schematic illustration of the proposed working mechanism underlying the memristive switching performance of oriented DNA. The oriented one-dimensional DNA chains provided effective ionic pathways, and the pre-anchored AgNPs along the DNA chains also helped guide the growth of filaments. **b)** Grazing-incidence small-angle scattering pattern of DNA layer prepared by electrophoretic deposition. **c)** Transmission electron microscopy image of the virgin state of the memristor with an oriented DNA structure. **d)** Transmission electron microscopy image of the set state of the memristor with an oriented DNA structure. Scale bars in **c** and **d**, 10 nm. **e)** Grazing-incidence small-angle scattering pattern of DNA layer prepared by dip coating. **f-g)** *I-V* characteristics of the DNA-bridged memristor with and without DNA orientation, respectively.

10.1002/ange.202004333

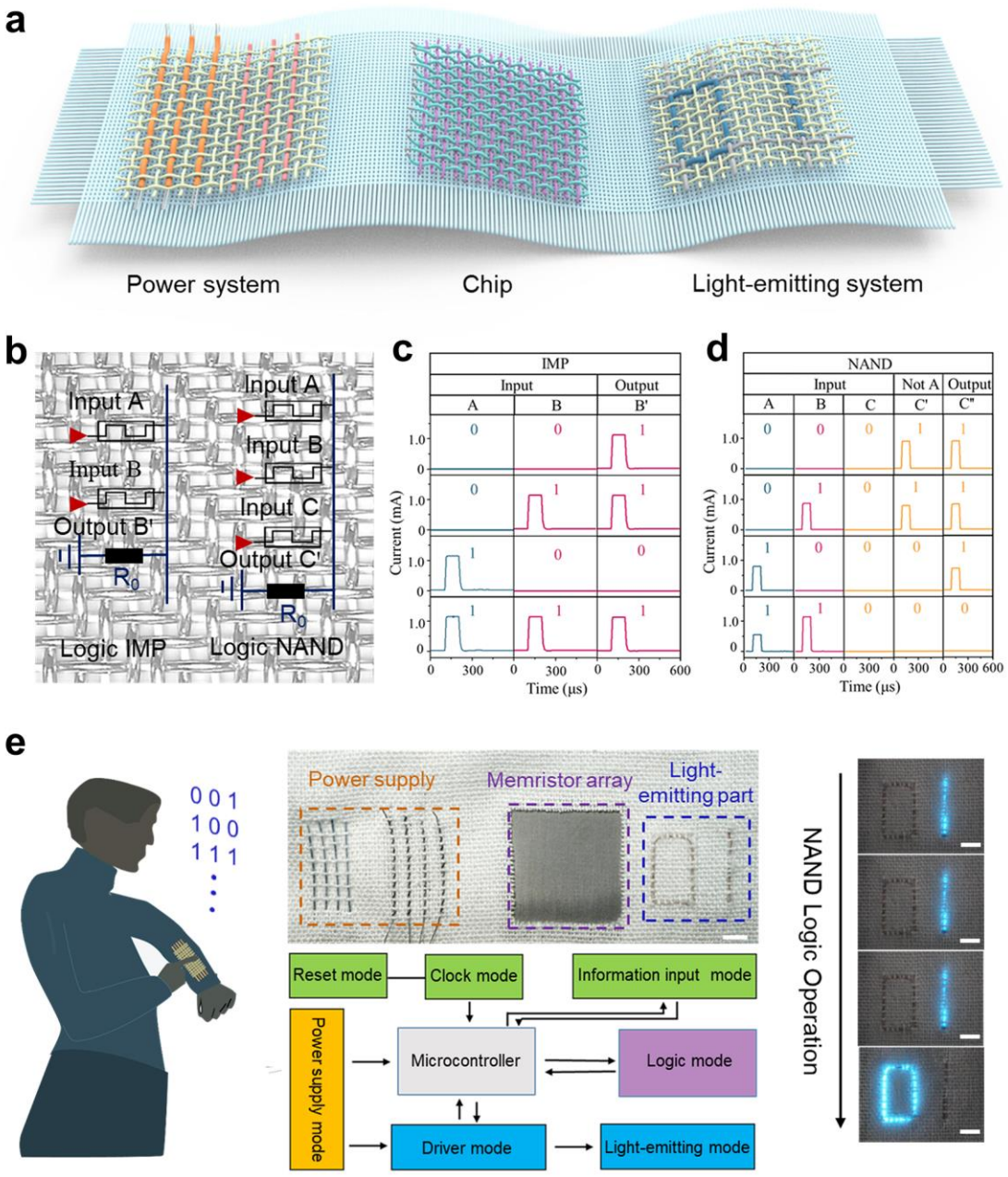

Figure 4. Demonstration of all-fabric information processing system with power-supplying, data processing and light-emitting modules. a) Schematic illustration of the integration of textile-type power supply, chip and light-emitting modules. **b)** Photograph of textile memristor cross-bar arrays. **c-d)** Demonstrations of the basic logic-in-memory function of IMP and NAND, respectively. **e)** Photograph and the operation mechanism of a proof-of-concept all-fabric data-processing system. Scale bars in **e** is 0.5 cm.

10.1002/ange.202004333

The Table of Contents

A metal fiber with oriented deoxyribonucleic acid molecules and Ag nanoparticles assembled on the surface as active layer is crossed with another metal fiber to produce new textile memristor. It shows the best-in-class performances, e.g., both ultra-low operation voltage of ~0.3 V and power consumption of ~100 pW and ultra-high switching speed of 20 ns, which exceed previous organic memristors.